Robust Fault-Tolerant Control for Underactuated Takeoff and Landing UAVs

YAO ZOU
University of Science and Technology Beijing, Beijing, China

KEWEI XIA
Ulsan National Institute of Science and Technology, Ulsan, South Korea

This article surveys the trajectory tracking issue of underactuated vertical takeoff and landing (VTOL) unmanned aerial vehicles (UAVs) subject to thrust and torque faults, i.e., loss of efficiency and actuator biases. In particular, a robust control algorithm against time-varying faults and disturbances is proposed. To exploit the underactuated nature of the VTOL UAV system, the control algorithm is developed based on a hierarchical framework, under which the position and attitude loops are studied in sequence. Specifically, by implementing a novel robust fault-tolerant control strategy, a force command is first synthesized for the position tracking to the desired trajectory, and then, a desired torque using an innovative sliding manifold is designed such that the nonsingular attitude tracking to an attitude command is achieved. This attitude command, as well as the desired thrust, is extracted from the synthesized force command. In terms of hierarchical system stability theory, it is shown that the overall closed-loop error system is asymptotically stable. Finally, simulation results validate and highlight the tracking performance of the proposed control algorithm.

Manuscript received March 28, 2019; revised July 9, 2019, October 5, 2019, and February 6, 2020; released for publication February 7, 2020. Date of publication March 16, 2020; date of current version October 9, 2020.

DOI. No. 10.1109/TAES.2020.2975446

Refereeing of this contribution was handled by J. Marzat.

This work was supported in part by the National Natural Science Foundation of China under Grant 61703229 and Grant 61806183, in part by the Fundamental Research Funds for the China Central Universities of the University of Science and Technology Beijing under Grant FRF-TP-19-018A3 and Grant FRF-TP-19-006B1, and in part by the Scientific and Technological Innovation Foundation of Shunde Graduate School, University of Science and Technology Beijing.

Authors' addresses: Yao Zou is with the School of Automation and Electrical Engineering and the Institute of Artificial Intelligence, University of Science and Technology Beijing, Beijing 100083, China, E-mail: (zouyao@ustb.edu.cn); Kewei Xia is with the School of Mechanical, Aerospace and Nuclear Engineering, Ulsan National Institute of Science and Technology, Ulsan 44919, South Korea, E-mail: (kwxia134@gmail.com). *(Corresponding author: Kewei Xia.)*

I. INTRODUCTION

With the rapid development of unmanned aerial vehicles (UAVs), they have been widely applied in military and civil areas [1]–[4]. As a typical representative, vertical take-off and landing (VTOL) UAVs have been of increasing interest recently, since they are available for some peculiar scenarios, where hovering or low-altitude/low-speed flights are required. Nonetheless, the VTOL UAV is inherently an underactuated nonlinear system that is sensitive to internal uncertainties and external disturbances [5]. Therefore, it is necessary to develop high-robustness control algorithms for the VTOL UAV system.

To explore the underactuated nature of the VTOL UAV system in a cascaded structure, i.e., three-degree-of-freedom (dof) translation motions and three-dof rotation motions driven by four independent controls, the hierarchical strategy is a viable control scheme [6], which is of a two-stage architecture composed of a "low-level" inner attitude loop and a "high-level" outer position loop [5]. Based on such a hierarchical strategy, various control schemes have been developed [7]–[12]. In particular, by integrating the backstepping technique and the proportional–derivative approach, a control scheme was proposed in [7] such that the bounded tracking was achieved while maintaining the position within a prescribed region. By introducing an immersion and invariance methodology for inertia parameter estimations, three adaptive controllers were developed in [9]–[11] to realize the asymptotic tracking. Moreover, in [12], the integral predictive controller and the nonlinear H_∞ controller were synthesized, respectively, for the position and attitude loops, while these two controllers were robust against parametric uncertainties and external disturbances. Furthermore, by implementing the hierarchical strategy, the tracking objective has also been fulfilled in the coordinated control of a team of VTOL UAVs [13]–[15]. However, there exists the singular problem when the attitude is represented by Euler angles [7]–[10], [12]. The control schemes in these references are based on a hypothesis that such singularity cannot occur during the tracking, but have no idea how to maintain it. In spite of some control approaches for singularity avoidance [16], [17], they are switching such that the resulting controllers are discontinuous. On the other hand, the control schemes proposed in [7]–[15] are available under the hypothesis that there exist no mechanical faults on the UAV actuators. In practice, the VTOL UAV is frequently encountered with unexpected rotor faults, such as failure, loss of efficiency, or bias, arising from aging and long-term friction. Such faults may degrade the tracking performance, invalidate the controller, or even deteriorate the system stability.

To address the issue caused by these actuator faults, the fault-tolerant control approach is available [18]. Generally, fault-tolerant control methods are categorized into active, passive, and their mixed ones [19]. The intuition behind the active fault-tolerant control lies in that a fault detection and diagnosis mechanism is first constructed to detect and identify the fault, and then, the fault information is online

recovered to reconfigure the controller [20], [21]. In terms of such an active idea, several fault-tolerant control schemes for VTOL UAVs were designed in [22]–[25]. On the other hand, the main idea behind the passive fault-tolerant control is to develop an individual controller that is inherently robust against the actuator faults. Compared with the passive fault-tolerant control, the system performance driven by the active fault-tolerant control could be deteriorated if the fault is not detected properly and rapidly [26]. In particular, by implementing the passive idea, an adaptive fault-tolerant control approach was proposed in [27] for the VTOL UAV such that the accurate trajectory tracking was realized. Nonetheless, the actuator faults considered there are constant.

This article develops a robust fault-tolerant control algorithm for the VTOL UAV subject to thrust and torque faults, as well as external disturbances such that it is capable of achieving the trajectory tracking objective. Under the hierarchical framework, the position and attitude loops are exploited by using novel passive fault-tolerant control schemes, where robust schemes are introduced to offset the effects arising from the rotor faults and external disturbances. In terms of hierarchical system stability theory, it is shown that the tracking errors driven by the proposed control algorithm asymptotically converge to zero. Compared with the previous works, the main contributions in this article are as follows. First, in contrast to [7]–[15], for the trajectory tracking of VTOL UAVs without any faults, the actuator faults are considered in this article. To counteract the fault effects, novel fault-tolerant control schemes are designed for the position and attitude loops, which, unlike [27], are robust against time-varying multiplicative and additive actuator faults, as well as external disturbances. Specifically, a robust strategy introducing smooth hyperbolic tangent functions is designed to compensate the upper bounds of these uncertainties. This effectively avoids a chattering phenomenon while guaranteeing the tracking precision. Next, unlike [7]–[10] and [12], where singularity is assumed not to occur in the attitude tracking when the attitude is represented by Euler angles, a continuous nonsingular attitude tracking control scheme, rather than the discontinuous ones [16], [17], is proposed herein. In particular, an innovative sliding manifold is first introduced such that the nonsingular attitude tracking is guaranteed provided that the sliding manifold is asymptotically stable. Then, a desired torque with an initial condition is proposed to asymptotically stabilize the specified sliding manifold. Finally, the asymptotic stability of the overall closed-loop error system is analyzed by using hierarchical system stability theory.

The rest of this article is arranged as follows. Some useful preliminaries are provided in Section II. The problem to be solved is stated in Section III. The main results, including the control algorithm development and stability analysis, are introduced in Section IV. Simulations are carried out in Section V to validate the developed control algorithm. Finally, Section VI concludes this article.

II. PRELIMINARIES

A. Notations

In what follows, $\mathbb{R}$ denotes real numbers, $\mathbb{R}^n$ denotes real vectors of dimension n, I_3 is a 3×3 unit matrix, $\lambda_{\min}(\cdot)$ and $\lambda_{\max}(\cdot)$ are the minimum and maximum eigenvalues of a square matrix, respectively, $\|\cdot\|_1$, $\|\cdot\|$, and $\|\cdot\|_\infty$ are the 1-norm, 2-norm, and ∞-norm of a vector,. respectively, and $\mathrm{diag}\{x_1, x_2, \ldots, x_n\}$ is a diagonal matrix with diagonal entries as scalars x_1 to x_n. For $x = [x_1, x_2, \ldots, x_n]^T$, define $\mathbf{tanh}(x) = [\tanh(x_1), \tanh(x_2), \ldots, \tanh(x_n)]^T$, $\int_0^x \mathbf{tanh}^T(\chi)\mathrm{d}\chi = \sum_{i=1}^n \int_0^{x_i} \tanh(\chi)\mathrm{d}\chi$, and $\mathbf{Tanh}(x) = \mathrm{diag}\{\tanh(x_1), \tanh(x_2), \ldots, \tanh(x_n)\}$. Moreover, superscript "$\times$" defines a transformation from $x = [x_1, x_2, x_3]^T$ to a skew-symmetric matrix

$$x^\times = \begin{bmatrix} 0 & -x_3 & x_2 \\ x_3 & 0 & -x_1 \\ -x_2 & x_1 & 0 \end{bmatrix}.$$

In addition, define $\mathcal{L}_2 = \{f : \mathbb{R}^+ \to \mathbb{R}^n | f$ is locally integrable, $\int_0^\infty \|f(t)\|\mathrm{d}t < \infty\}$, and $\mathcal{L}_\infty = \{f : \mathbb{R}^+ \to \mathbb{R}^n | f$ is locally integrable, $\mathrm{ess\,sup}_{t\in\mathbb{R}^+} \|f(t)\| < \infty\}$.

B. Useful Lemmas

LEMMA 1 (SEE [28]) The hyperbolic tangent function $\tanh(x)$ satisfies

$$\int_0^x \tanh(\chi)\mathrm{d}\chi \le \frac{x^2}{2}. \tag{1}$$

LEMMA 2 (SEE [7]) The following inequality holds for $x \in (-k, k)$:

$$\ln \frac{k^2}{k^2 - x^2} \le \frac{x^2}{k^2 - x^2}. \tag{2}$$

LEMMA 3 (SEE [29]) The following inequality holds for $x \in \mathbb{R}$ and $\eta > 0$:

$$|x| - x\tanh\left(\frac{x}{\eta}\right) \le k_q\eta \tag{3}$$

where $k_q = 0.2785$ satisfies $k_q = e^{-k_q - 1}$.

III. PROBLEM STATEMENT

A. System Model

The VTOL UAV is considered as a six-dof rigid body and is modeled in two basic frames: earth frame $\mathcal{E} = \{O_E x_E y_E z_E\}$ whose origin is posited at a fixed point on the earth with the north-east-ground axes, and body frame $\mathcal{B} = \{O_B x_B y_B z_B\}$ whose origin is chosen as the airframe center with the forward-left-upward axes. By neglecting the earth motion, frame $\mathcal{E}$ can be regarded as an inertial reference. In terms of the Newton–Euler formulation [7], the VTOL UAV model is formulated by

$$\dot{p} = v \tag{4}$$

$$m\dot{v} = -mge_3 + \bar{T}Re_3 + d_f \tag{5}$$

$$\Theta\dot{\gamma} = \omega \tag{6}$$

$$J\dot{\omega} = -\omega^{\times}J\omega + \bar{\tau} + d_{\tau} \tag{7}$$

where $p = [p_x, p_y, p_z]^T$ and $v = [v_x, v_y, v_z]^T$ denote the position and velocity of the airframe center in frame $\mathcal{E}$, respectively, m denotes the total mass, g denotes the local gravitational acceleration, $e_3 \triangleq [0, 0, 1]^T$, $\bar{T}$ denotes the applied thrust along axis z_B, $R = R(\gamma) \in \mathrm{SO}(3)$ denotes the rotation matrix from frame $\mathcal{B}$ to frame $\mathcal{E}$, $\gamma = [\phi, \theta, \psi]^T$ denotes the Euler angle vector (i.e., roll, pitch, and yaw) characterizing the UAV attitude, $\Theta = \Theta(\gamma)$ is a matrix parameterized by γ, $\omega = [\omega_x, \omega_y, \omega_z]^T$ denotes the angular velocity of the UAV in frame $\mathcal{B}$, $J = \mathrm{diag}\{J_x, J_y, J_z\}$ denotes the inertia matrix with respect to frame $\mathcal{B}$, $\bar{\tau}$ denotes the applied torque in frame $\mathcal{B}$, and d_f, d_τ denote the disturbance force and torque, respectively.

Moreover, motivated by [30], the rotation matrix R results from three consecutive rotations of frame $\mathcal{B}$ by $\phi - \theta - \psi$ with respect to the corresponding frames to frame $\mathcal{E}$. Hence, R is explicitly parameterized by γ according to

$$R(\gamma) = \begin{bmatrix} \mathrm{c}\theta\mathrm{c}\psi & \mathrm{s}\phi\mathrm{s}\theta\mathrm{c}\psi - \mathrm{c}\phi\mathrm{s}\psi & \mathrm{c}\phi\mathrm{s}\theta\mathrm{c}\psi + \mathrm{s}\phi\mathrm{s}\psi \\ \mathrm{c}\theta\mathrm{s}\psi & \mathrm{s}\phi\mathrm{s}\theta\mathrm{s}\psi + \mathrm{c}\phi\mathrm{c}\psi & \mathrm{c}\phi\mathrm{s}\theta\mathrm{s}\psi - \mathrm{s}\phi\mathrm{c}\psi \\ -\mathrm{s}\theta & \mathrm{s}\phi\mathrm{c}\theta & \mathrm{c}\phi\mathrm{c}\theta \end{bmatrix}$$

where $\mathrm{c}(\cdot)$ and $\mathrm{s}(\cdot)$ are short for $\cos(\cdot)$ and $\sin(\cdot)$, respectively. In addition, the matrix Θ and its derivative are expressed by

$$\Theta(\gamma) = \begin{bmatrix} 1 & 0 & -\mathrm{s}\theta \\ 0 & \mathrm{c}\phi & \mathrm{s}\phi\mathrm{c}\theta \\ 0 & -\mathrm{s}\phi & \mathrm{c}\phi\mathrm{c}\theta \end{bmatrix}$$

$$\dot{\Theta}(\gamma, \dot{\gamma}) = \begin{bmatrix} 0 & 0 & -\dot{\theta}\mathrm{c}\theta \\ 0 & -\dot{\phi}\mathrm{s}\phi & \dot{\phi}\mathrm{c}\phi\mathrm{c}\theta - \dot{\theta}\mathrm{s}\phi\mathrm{s}\theta \\ 0 & -\dot{\phi}\mathrm{c}\phi & -\dot{\phi}\mathrm{s}\phi\mathrm{c}\theta - \dot{\theta}\mathrm{c}\phi\mathrm{s}\theta \end{bmatrix}.$$

Due to the fact that $\det\Theta = \cos\theta$, Θ is invertible if the pitch θ is located within $(-\pi/2, \pi/2)$.

B. Thrust and Torque Faults

Generally, the applied thrust and torque driving the VTOL UAV are generated by a group of rotors. However, subject to adverse factors ranging from internal mechanical hitch (e.g., aging or friction) to external harsh environment (e.g., dusty wind or electromagnetic interference), it is hard to maintain well-running rotor actuators in practice. This, therefore, will bring in partial failure and further faults in the applied force and torque. Without taking these potential faults into account, the resulting applied thrust and torque may lead to performance demotion or even instability of the controlled UAV.

Suppose that the applied force and torque simultaneously suffer from multiplicative and additive faults. In particular, they are formulated by

$$\bar{T} = (1 - \varepsilon)T_n + T_d \tag{8}$$

$$\bar{\tau} = (I_3 - \Upsilon)\tau_n + \tau_d \tag{9}$$

where T_n and τ_n denote the desired thrust and torque to be designed, respectively, $\varepsilon \in [0, 1)$ and $\Upsilon = \mathrm{diag}\{\epsilon_x, \epsilon_y, \epsilon_z\}$ with $\epsilon_i \in [0, 1)$, $i = x, y, z$, denote the actuator efficiency factors, and T_d and τ_d denote the actuator biases. Note that $\varepsilon = 0$, $T_d = 0$ and $\Upsilon = 0_3$, $\tau_d = 0$ correspond to the nominal case free of faults.

Substituting (8) into (5) and (9) into (7) yields

$$\dot{v} = -ge_3 + \frac{T_n}{m}Re_3 + \rho_T + \rho_p \tag{10}$$

$$J\dot{\omega} = -\omega^{\times}J\omega + \tau_n + \rho_\tau + \rho_a \tag{11}$$

where $\rho_T = -\varepsilon T_n Re_3/m$ and $\rho_\tau = -\Upsilon\tau_n$ are perturbations caused by multiplicative faults, and $\rho_p = (T_d Re_3 + d_f)/m$ and $\rho_a = \tau_d + d_\tau$ are lumped perturbations arising from additive faults and external disturbances. Note that since the thrust and torque faults and disturbances are time-varying and unknown, so are ρ_T, ρ_τ, ρ_p, and ρ_a.

REMARK 1 To exemplify the actuator faults on the VTOL UAV, a quadcopter is considered. Its applied force $\bar{T}$ and torque $\bar{\tau}$ are generated by four equally spaced rotors according to

$$\begin{bmatrix} \bar{T} \\ \bar{\tau}_x \\ \bar{\tau}_y \\ \bar{\tau}_z \end{bmatrix} = \begin{bmatrix} 1 & 1 & 1 & 1 \\ 0 & -D & 0 & D \\ D & 0 & -D & 0 \\ C & -C & C & -C \end{bmatrix} \begin{bmatrix} f_1 \\ f_2 \\ f_3 \\ f_4 \end{bmatrix} \tag{12}$$

where D is the distance from the quadcopter c.g. to the rotation axis of each rotor, C is the antitorque coefficient, and f_j ($j = 1, 2, 3, 4$) is the thrust generated by each rotor. Suppose that the symmetric rotors, i.e., rotors 1 and 3, suffer from the loss of efficiency and actuator biases arising from the fluctuation caused by the loose joint. Specifically, we have

$$f_1 = (1 - \varepsilon)f_{1,n} + f_{1,d} \tag{13}$$

$$f_3 = (1 - \varepsilon)f_{3,n} + f_{3,d} \tag{14}$$

where $f_{1,n}$ and $f_{3,n}$ denote the desired rotor thrusts, $\varepsilon \in [0, 1)$ denotes the actuator efficiency factor, and $f_{1,d}$ and $f_{3,d}$ denote the actuator biases. By substituting (12)–(14) into (5) and (7), we can also obtain (10) and (11) with $T_n = f_{1,n} + f_2 + f_{3,n} + f_4$,

$$\tau_n = \begin{bmatrix} 0 & -D & 0 & D \\ D & 0 & -D & 0 \\ C & -C & C & -C \end{bmatrix} \begin{bmatrix} f_{1,n} \\ f_2 \\ f_{3,n} \\ f_4 \end{bmatrix}$$

$\rho_T = \varepsilon_1(f_{1,n} + f_{3,n})Re_3/m$, $\rho_p = ((f_{1,d} + f_{3,d})Re_3 + d_f)/m$, $\rho_\tau = -\varepsilon[0, D(f_{1,n} - f_{3,n}), C(f_{1,n} + f_{3,n})]^T$, and $\rho_a = [0, D(f_{1,d} - f_{3,d}), C(f_{1,d} + f_{3,d})]^T + d_\tau$.

C. Control Objective

Given a smooth reference trajectory $p_r = [p_{r,x}, p_{r,y}, p_{r,z}]^T$ and yaw ψ_r, we intend to develop desired thrust T_n

and torque τ_n for the VTOL UAV (4)–(7) subject to thrust and torque faults (8) and (9) such that it can track p_r and ψ_r. In particular, we have

$$\lim_{t\to\infty}(p(t)-p_r(t))=0,\ \lim_{t\to\infty}(\psi(t)-\psi_r(t))=0. \quad (15)$$

Suppose that the concerned VTOL UAV has access to its full states including position, velocity, attitude, and angular velocity via corresponding measurement devices. The time-varying actuator faults and disturbances have adverse effects on the tracking performance in practice. To guarantee that the control algorithm is robust against these uncertainties, a fault-tolerant scheme is to be explored in this article. For the sake of its feasibility, some fundamental assumptions are made as follows.

ASSUMPTION 1 There exist constants $\bar{\varepsilon}\in[0,\sqrt{3}/3)$ and $\bar{\epsilon}\in[0,1)$ such that the actuator efficiency factors ε and Υ satisfy

$$\varepsilon\in[0,\bar{\varepsilon}),\ \epsilon_i\in[0,\bar{\epsilon}),\ i=x,y,z. \quad (16)$$

ASSUMPTION 2 The lumped perturbations ρ_p and ρ_a are bounded by

$$|\rho_{p,i}|\le\bar{\rho}_{p,i},\ |\rho_{a,i}|\le\bar{\rho}_{a,i},\ i=x,y,z \quad (17)$$

where $\bar{\rho}_p=[\rho_{p,x},\rho_{p,y},\rho_{p,z}]^T$ and $\bar{\rho}_a=[\rho_{a,x},\rho_{a,y},\rho_{a,z}]^T$ are constant bound vectors.

REMARK 2 In practice, too serious multiplicative faults lead to uncontrollability of the VTOL UAVs, since inadequate power is insufficient to support their flights. To this end, Assumption 1, as a fault recoverability assessment [32], guarantees the controllability of the VTOL UAVs by using the proposed control algorithm. In addition, the external disturbances and additive faults cannot be arbitrarily large in reality, thereby leading to the viability of Assumption 2. In addition, as will be shown subsequently, large upper bounds $\bar{\varepsilon}$, $\bar{\epsilon}$, $\bar{\rho}_p$, and $\bar{\rho}_a$ are beneficial for improving the robust performance of the proposed control algorithm against the unknown actuator faults and disturbances.

REMARK 3 Unlike [1], [6], [11], and [14], in which just the trajectory tracking is studied, we also consider the yaw tracking into the control objective (15). Such yaw tracking is of practical significance, which facilitates the aerial surveillance, reconnaissance, and other missions.

IV. CONTROL ALGORITHM DEVELOPMENT

To solve the trajectory tracking problem of the underactuated VTOL UAV system, the hierarchical strategy is available. Specifically, a force command is first synthesized in the position loop. The desired thrust and an attitude command, as a result of the magnitude and orientation of the force command, are then extracted, respectively. Next, a desired torque is developed in the attitude loop for the tracking to the attitude command. Under such a hierarchical framework, the control algorithm process is specified as follows [11]. In the first place, the trajectory tracking problem of the VTOL UAV system is converted into the stabilization problem of its associated error system. Next, a force command and a desired torque are synthesized in sequence such that the position and attitude error systems are asymptotically stable. Eventually, the stability analysis of the overall closed-loop error system is undertaken based on hierarchical system stability theory.

A. Problem Conversion

Define the position error $p_e=[p_{e,x},p_{e,y},p_{e,z}]^T=p-p_r$ and the velocity error $v_e=[v_{e,x},v_{e,y},v_{e,z}]^T=v-\dot{p}_r$. By virtue of (4) and (10), the position error system satisfies

$$\dot{p}_e=v_e \quad (18a)$$

$$\dot{v}_e=-ge_3-\ddot{p}_r+u_c+\rho_T+\rho_p+\frac{T_n}{m}(R-R_c)e_3 \quad (18b)$$

where $u_c=T_nR_ce_3/m$ is the force command and

$$R_c=R_c(\gamma_c)=\begin{bmatrix}c\theta_c c\psi_r & s\phi_c s\theta_c c\psi_r-c\phi_c s\psi_r & c\phi s\theta_c c\psi_r+s\phi_c s\psi_r\\ c\theta_c s\psi_r & s\phi_c s\theta_c s\psi_r+c\phi_c c\psi_r & c\phi_c s\theta_c s\psi_r-s\phi c\psi_r\\ -s\theta_c & s\phi_c c\theta_c & c\phi_c c\theta_c\end{bmatrix}$$

is the rotation matrix command with $\gamma_c=[\phi_c,\theta_c,\psi_r]^T$ being the Euler angle command vector and ϕ_c as well as θ_c being the roll and pitch commands. Note that the position error system (18) can be treated as a nominal system

$$\dot{p}_e=v_e \quad (19a)$$

$$\dot{v}_e=-ge_3-\ddot{p}_r+u_c+\rho_T+\rho_p \quad (19b)$$

perturbed by $T_n(R-R_c)e_3/m$. Moreover, due to the fact that $\|R_ce_3\|=1$, once the force command u_c is determined, the desired thrust can be immediately derived as

$$T_n=m\|u_c\|. \quad (20)$$

Since we implement a hierarchical framework to exploit the underactuated nature of the VTOL UAV system, it is necessary to extract the roll command ϕ_c and pitch command θ_c from the force command u_c. They, together with the reference yaw ψ_r, serve as the attitude tracking objective. According to [7], if the force command $u_c=[u_{c,x},u_{c,y},u_{c,z}]^T$ given in the position error system (18) satisfies $u_{c,z}\neq 0$, the roll command ϕ_c and pitch command θ_c can be extracted as

$$\begin{cases}\phi_c=\arcsin\left(\frac{u_{c,x}\sin\psi_r-u_{c,y}\cos\psi_r}{\|u_c\|}\right), & \phi_c\in\left(-\frac{\pi}{2},\frac{\pi}{2}\right)\\ \theta_c=\arctan\left(\frac{u_{c,x}\cos\psi_r+u_{c,y}\sin\psi_r}{u_{c,z}}\right), & \theta_c\in\left(-\frac{\pi}{2},\frac{\pi}{2}\right).\end{cases} \quad (21)$$

Next, define the attitude error $\gamma_e=[\phi_e,\theta_e,\psi_e]^T=\gamma-\gamma_c$. By virtue of (6) and (11), the attitude error system is derived as

$$J(\dot{\Theta}\dot{\gamma}_e+\Theta\ddot{\gamma}_e)=-\omega^{\times}J\omega-J(\dot{\Theta}\dot{\gamma}_c+\Theta\ddot{\gamma}_c)+\tau_n+\rho_\tau+\rho_a. \quad (22)$$

In terms of the above argument, the trajectory tracking problem of the VTOL UAV system (4)–(7) can be converted into the stabilization problem of the error system (18) and (22). We use a lemma to elaborate this point.

PROPOSITION 1 Consider the error system (18) and (22). If a force command u_c and a desired torque τ_n can be synthesized such that $\lim_{t\to\infty} p_e(t) = 0$, $\lim_{t\to\infty} v_e(t) = 0$, $\lim_{t\to\infty} \gamma_e(t) = 0$ and $\lim_{t\to\infty} \dot{\gamma}_e(t) = 0$, the trajectory tracking of the VTOL UAV system (4)–(7) is achieved in the sense of (15).

B. Force Command Synthesis

We next focus on the synthesis of a force command such that the position error system (18) is stabilized, where a robust control scheme is designed to address the perturbations caused by the time-varying faults and disturbances. On the other hand, in order for nonsingularity in the attitude command extraction (21), the nonsingular condition $u_{c,z} \neq 0$ should be considered when synthesizing the force command.

Define a manifold surface $s_p = [s_{p,x}, s_{p,y}, s_{p,z}]^T = c_p p_e + v_e$ with $c_p > 0$. For the purpose of stabilizing the position error system, we propose a force command in the following form:

$$u_c = u_{\text{nom}} + u_{p,1} + u_{p,2} \tag{23}$$

$$u_{\text{nom}} = ge_3 + \ddot{p}_r - k_p(\mathbf{tanh}(s_p) + \mathbf{tanh}(v_e)) \tag{23a}$$

$$u_{p,1} = -\frac{\sqrt{3}\bar{\varepsilon}}{\sqrt{3} - 3\bar{\varepsilon}} \varrho_p \mathbf{tanh}\left(\frac{\vartheta_p}{\eta}\right) \tag{23b}$$

$$u_{p,2} = -\mathbf{Tanh}\left(\frac{\vartheta_p}{\eta}\right) \bar{\rho}_p \tag{23c}$$

where k_p is a positive control parameter, $\eta(t) = e^{-\alpha t}$ with $\alpha > 0$, $\vartheta_p = [\vartheta_{p,x}, \vartheta_{p,y}, \vartheta_{p,z}]^T = \mathbf{tanh}(s_p) + \mathbf{tanh}(v_e) + c_p v_e/k_p$, $\varrho_p = \|u_{\text{nom}} + u_{p,2}\|$, and $\bar{\varepsilon}$, $\bar{\rho}_p$ are the constants introduced in Assumptions 1 and 2. Note from (23) that the proposed force command consists of two items. The first item, i.e., u_{nom}, is a nominal component, where the saturated hyperbolic tangent function is introduced for the sake of the subsequent parameter choice such that the nonsingular condition $u_{c,z} \neq 0$ is guaranteed. The second item, including $u_{p,1}$ and $u_{p,2}$, is a robust component against the thrust fault and disturbance force.

Moreover, in order to warrant the nonsingular condition $u_{c,z} \neq 0$, it is necessary to choose the control parameter k_p carefully. Motivated by this fact, the following proposition proposes a sufficient condition for the existence of k_p such that $u_{c,z} > 0$ is guaranteed all the time.

PROPOSITION 2 Consider the proposed force command (23). Suppose that Assumptions 1 and 2 hold with the reference acceleration $\ddot{p}_r$ and the bound constants $\bar{\varepsilon}$, $\bar{\rho}_p$ satisfying

$$\bar{\varepsilon} < \frac{\sqrt{3} - 1}{2}, \varsigma \sup_{t\geq 0} \|\dddot{p}_r(t)\| + \sup_{t\geq 0} |\ddot{p}_{r,z}(t)| + (1 + \varsigma)\|\bar{\rho}_p\| < g \tag{24}$$

where $\varsigma = \bar{\varepsilon}/\sqrt{2\bar{\varepsilon}^2 - 2\sqrt{3}\bar{\varepsilon} + 1}$ and $\bar{p}_r = [p_{r,x}, p_{r,y}]^T$. If the control parameter k_p satisfies

$$k_p < \frac{1}{2 + 2\sqrt{2}\varsigma}\left[g - \sup_{t\geq 0} |\ddot{p}_{r,z}(t)| - \varsigma \sup_{t\geq 0} \|\dddot{p}_r(t)\| - (1 + \varsigma)\|\bar{\rho}_p\|\right] \tag{25}$$

then $u_{c,z}(t) > 0$, $\forall t \geq 0$ is guaranteed.

PROOF See the Appendix. ■

REMARK 4 Note from Proposition 2 that the established selection criterion for the control parameter k_p is irrelative to the system states. In other words, given (24), as long as the control parameter k_p is chosen according to (25), the VTOL UAV can be initialized arbitrarily without violating the nonsingular condition $u_{c,z} \neq 0$. On the other hand, note that the right-hand side of (25) is decreasing as ε and $\|\bar{\rho}_p\|$ decrease. This indicates that, if more knowledge about small actuator faults and disturbances is available, the choices of the upper bounds ε and $\bar{\rho}_p$ become less conservative, thereby leading to the less conservative choice of the control parameter k_p.

C. Desired Torque Synthesis

In what follows, we intend to synthesize a desired torque such that the attitude error system (22) is stabilized asymptotically. As mentioned above, singularity occurs at $\theta = \pm\pi/2$ for the Euler attitude representation. Accordingly, the synthesized desired torque should ensure $\theta \in (-\pi/2, \pi/2)$ in case of singularity.

For the purpose of maintaining $\theta \in (-\pi/2, \pi/2)$, we introduce a manifold surface $s_a = [s_{a,x}, s_{a,y}, s_{a,z}]^T$ in the following form:

$$s_a = \dot{\gamma}_e + [c_a(I_3 + \Gamma_1) + \Gamma_2]\gamma_e \tag{26}$$

where $c_a > 0$, $\Gamma_1 = \text{diag}\{0, 1/(k_\theta^2 - \theta_e^2), 0\}$, and $\Gamma_2 = \text{diag}\{0, |\dot{k}_\theta/k_\theta|, 0\}$ with $k_\theta = \pi/2 - |\theta_c|$. By virtue of (22), the dynamics of s_a can be derived as

$$\begin{aligned} J\frac{d}{dt}(\Theta s_a) &= J(\dot{\Theta}s_a + \Theta\dot{s}_a) \\ &= J\left\{\dot{\Theta}\dot{\gamma}_e + \Theta\ddot{\gamma}_e + \dot{\Theta}[c_a(I_3 + \Gamma_1) + \Gamma_2]\gamma_e \right. \\ &\quad \left. + \Theta(c_a\dot{\Gamma}_1 + \dot{\Gamma}_2)\gamma_e + \Theta[c_a(I_3 + \Gamma_1) + \Gamma_2]\dot{\gamma}_e\right\} \\ &= -\omega^\times J\omega + J\varpi + \tau_n + \rho_\tau + \rho_a \end{aligned} \tag{27}$$

where $\varpi = \Theta[c_a(I_3 + \Gamma_1) + \Gamma_2]\dot{\gamma}_e + [\dot{\Theta}(c_a(I_3 + \Gamma_1) + \Gamma_2) + \Theta(c_a\dot{\Gamma}_1 + \dot{\Gamma}_2)]\gamma_e - (\dot{\Theta}\dot{\gamma}_c + \Theta\ddot{\gamma}_c)$. For the sake of the attitude tracking, we propose a desired torque as follows:

$$\tau_n = \tau_{\text{nom}} + \tau_{a,1} + \tau_{a,2} \tag{28}$$

$$\tau_{\text{nom}} = \omega^\times J\omega - J\varpi - k_a\Theta^{-T}s_a \tag{28a}$$

$$\tau_{a,1} = -\frac{\bar{\epsilon}}{1 - \bar{\epsilon}}\Psi_a \mathbf{tanh}\left(\frac{\Psi_a\Theta s_a}{\eta}\right) \tag{28b}$$

$$\tau_{a,2} = -\mathbf{Tanh}\left(\frac{\Theta s_a}{\eta}\right)\bar{\rho}_a \tag{28c}$$

where k_a is a positive control parameter, $\Psi_a = \text{diag}\{|\varrho_{a,x}|, |\varrho_{a,y}|, |\varrho_{a,z}|\}$ with $\varrho_a = \tau_{\text{nom}} + \tau_{a,2}$, and η has been defined below (23).

REMARK 5 Note from the proposed force command (23) and desired torque (28) that increasing the upper bounds $\bar{\varepsilon}$, $\bar{\rho}_p$, $\bar{\epsilon}$, and $\bar{\rho}_a$ can effectively improve the robustness performance against the actuator faults and external disturbances. However, too large $\bar{\varepsilon}$, $\bar{\rho}_p$, $\bar{\epsilon}$, and $\bar{\rho}_a$ may violate the input saturation constraint in practice. Therefore, appropriate upper bounds $\bar{\varepsilon}$, $\bar{\rho}_p$, $\bar{\epsilon}$, and $\bar{\rho}_a$ should be specified by considering the tradeoff between input saturation and robustness performance.

D. Stability Analysis

According to Proposition 1, the trajectory tracking of the VTOL UAV system (4)–(7) is achieved if only the evolved error system (18), (22) can be asymptotically stabilized. Note that the evolved error system (18), (22) is under a hierarchical framework. Accordingly, its stability is analyzed in terms of the hierarchical system stability theory [33]. In particular, the evolved error system (18), (22) can be asymptotically stabilized if following three conditions are guaranteed simultaneously.

- Th.i The nominal position error system (19) can be asymptotically stabilized by the proposed force command (23).
- Th.ii The attitude error system (22) can be asymptotically stabilized by the proposed desired torque (28).
- Th.iii The perturbation item $T_n(R - R_c)e_3/m$ in the position error system (18) asymptotically converges to zero.

We next show these three conditions in Propositions 3–5, respectively.

In the first place, Proposition 3 shows that the attitude tracking is fulfilled without singularity.

PROPOSITION 3 Consider the attitude error system (22). Suppose that Assumptions 1 and 2 hold. If the initial pitch $\theta(0)$ satisfies

$$-\frac{\pi}{2} + \max\{0, 2\theta_c(0)\} < \theta(0) < \frac{\pi}{2} + \min\{0, 2\theta_c(0)\} \tag{29}$$

the proposed desired torque (28) guarantees that $\lim_{t\to\infty} \gamma_e(0) = 0$ and $\lim_{t\to\infty} \dot{\gamma}_e(0) = 0$ without singularity, i.e., $\theta(t) \in (-\pi/2, \pi/2)$, $\forall t \geq 0$.

PROOF First, assign a Lyapunov function as follows:

$$L_a = \frac{1}{2}(\Theta s_a)^T J \Theta s_a. \tag{30}$$

Its derivative along (27) satisfies

$$\dot{L}_a = (\Theta s_a)^T(-\omega^\times J\omega + \tau_n + \rho_\tau + \rho_a). \tag{31}$$

Denote $\vartheta_a = \Theta s_a$. Given Assumptions 1 and 2 and the fact that $|\tau_{a,1,i}| \leq \bar{\epsilon}|\varrho_{a,i}|/(1-\bar{\epsilon})$, $i = x, y, z$, it follows from Lemma 1 that

$$\begin{aligned}
\vartheta_a^T \rho_\tau &\leq \bar{\epsilon} \sum_{i=x,y,z} |\vartheta_{a,i}||\tau_{c,i}| \leq \frac{\bar{\epsilon}}{1-\bar{\epsilon}} \sum_{i=x,y,z} |\vartheta_{a,i}||\varrho_{a,i}| \\
&\leq \frac{\bar{\epsilon}}{1-\bar{\epsilon}} \sum_{i=x,y,z} \left[\vartheta_{a,i}|\varrho_{a,i}| \tanh\left(\frac{\vartheta_{a,i}|\varrho_{a,i}|}{\eta}\right) + k_q\eta\right] \\
&= \frac{\bar{\epsilon}}{1-\bar{\epsilon}}(\Psi_a\vartheta_a)^T \mathbf{tanh}\left(\frac{\Psi_a\vartheta_a}{\eta}\right) + \frac{3k_q\eta\bar{\epsilon}}{1-\bar{\epsilon}} \\
\vartheta_a^T \rho_a &\leq \vartheta_a^T \mathbf{Tanh}\left(\frac{\vartheta_a}{\eta}\right)\bar{\rho}_a + k_q\eta\|\bar{\rho}_a\|_1.
\end{aligned}$$

Thus, $\dot{L}_a$ satisfies

$$\begin{aligned}
\dot{L}_a \leq (\Theta s_a)^T \Bigg[&-\omega^\times J\omega + \tau_n + \frac{\bar{\epsilon}}{1-\bar{\epsilon}}\Psi_a \mathbf{tanh}\left(\frac{\Psi_a\Theta s_a}{\eta}\right) \\
&+ \mathbf{Tanh}\left(\frac{\Theta s_a}{\eta}\right)\bar{\rho}_a\Bigg] + \hbar_a\eta
\end{aligned} \tag{32}$$

where $\hbar_a = 3k_q\bar{\epsilon}/(1-\bar{\epsilon}) + k_q\|\bar{\rho}_a\|_1$. By virtue of (30), substituting the proposed desired torque (28) into (32) yields

$$\dot{L}_a \leq -k_a\|s_a\|^2 + \hbar_a\eta \leq -\frac{2k_a}{\lambda_{\max}(J)\lambda_{\max}(\Theta^T\Theta)}L_a + \hbar_a\eta. \tag{33}$$

Due to the fact that the eigenvalues of $\Theta^T\Theta$ are $1 \pm \sin\theta$ and 1, we know that $\lambda_{\max}(\Theta^T\Theta) \leq 2$. It thus follows that

$$\dot{L}_a \leq -\bar{k}_a L_a + \hbar_a\eta \tag{34}$$

where $\bar{k}_a = k_a/\lambda_{\max}(J)$. According to the comparison principle [33], this implies that

$$L_a(t) \leq \begin{cases} e^{-\bar{k}_a t}L_a(0) + \frac{\hbar_a}{\bar{k}_a - \alpha}(e^{-\alpha t} - e^{-\bar{k}_a t}), & \text{if } \alpha \neq \bar{k}_a \\ e^{-\bar{k}_a t}L_a(0) + \frac{\hbar_a}{\bar{k}_a}e^{-\bar{k}_a t}t, & \text{if } \alpha = \bar{k}_a. \end{cases}$$

Hence, we have that $\lim_{t\to\infty} L_a(t) = 0$. If $\theta \in (-\pi/2, \pi/2)$, then $\lambda_{\min}(\Theta^T\Theta) > 0$. It then follows from (30) that $\lim_{t\to\infty} s_a(t) = 0$.

Next, in terms of (26), the dynamics of γ_e satisfies

$$\dot{\gamma}_e = -[c_a(I_3 + \Gamma_1) + \Gamma_2]\gamma_e + s_a. \tag{35}$$

Assign another Lyapunov function as follows:

$$L_\gamma = \frac{1}{2}\phi_e^2 + \frac{1}{2}\ln\frac{k_\theta^2}{k_\theta^2 - \theta_e^2} + \frac{1}{2}\psi_e^2. \tag{36}$$

Its derivative along (35) satisfies

$$\begin{aligned}
\dot{L}_\gamma &= \left[\phi_e, \frac{\theta_e}{k_\theta^2 - \theta_e^2}, \psi_e\right]\dot{\gamma}_e - \frac{\theta_e^2}{k_\theta^2 - \theta_e^2}\frac{\dot{k}_\theta}{k_\theta} \\
&= \left[\phi_e, \frac{\theta_e}{k_\theta^2 - \theta_e^2}, \psi_e\right](-c_a\gamma_e - c_a\Gamma_1\gamma_e + s_a) \\
&\quad + \frac{\theta_e^2}{k_\theta^2 - \theta_e^2}\left(\left|\frac{\dot{k}_\theta}{k_\theta}\right| - \frac{\dot{k}_\theta}{k_\theta}\right) \\
&\leq -c_a\left[\phi_e, \frac{\theta_e}{k_\theta^2 - \theta_e^2}, \psi_e\right]\gamma_e - c_a\frac{\theta_e^2}{(k_\theta^2 - \theta_e^2)^2} \\
&\quad + \left[\phi_e, \frac{\theta_e}{k_\theta^2 - \theta_e^2}, \psi_e\right]s_a
\end{aligned}$$

$$\leq -\frac{c_a}{2}\left[\phi_e, \frac{2\theta_e}{k_\theta^2-\theta_e^2}, \psi_e\right]\gamma_e - \frac{c_a}{2}\frac{\theta_e^2}{(k_\theta^2-\theta_e^2)^2} + \frac{1}{2c_a}\|s_a\|^2$$
$$\leq -\frac{c_a}{2}\left[\phi_e, \frac{\theta_e}{k_\theta^2-\theta_e^2}, \psi_e\right]\gamma_e + \frac{1}{2c_a}\|s_a\|^2. \quad (37)$$

According to Lemma 2, we know that $\ln(k_\theta^2/(k_\theta^2-\theta_e^2)) \leq \theta_e^2/(k_\theta^2-\theta_e^2)$. It thus follows from (36) that

$$\dot{L}_\gamma \leq -c_a L_\gamma + \frac{1}{2c_a}\|s_a\|^2. \quad (38)$$

For system $\dot{y} = -c_a y + \|s_a\|^2/(2c_1)$ with respect to $y \in [0, \infty)$, based on input-to-state stability theory [33], it follows that $\lim_{t\to\infty} y(t) = 0$ given the fact that $\lim_{t\to\infty} s_a(t) = 0$. According to the comparison principle [33], it follows that there exists a positive constant $\bar{L}_\gamma$ such that $L_\gamma(t) \leq \bar{L}_\gamma$, $\forall t \geq 0$, and further that $\lim_{t\to\infty} L_\gamma(t) = 0$. Thus, it can be concluded that $\lim_{t\to\infty} \gamma_e(t) = 0$. This, together with the fact that $\lim_{t\to\infty} s_a(t) = 0$, implies that $\lim_{t\to\infty} \dot{\gamma}_e(t) = 0$ given (35).

On the other hand, by virtue of (36), we know that $\ln(k_\theta^2/(k_\theta^2-\theta_e^2)) \leq 2\bar{L}_\gamma$. This indicates that $|\theta_e(t)| < k_\theta(t)$, $\forall t \geq 0$ as long as $|\theta_e(0)| < k_\theta(0)$. Moreover, it is trivial to show that $\theta(0)$ satisfying (29) implies $|\theta_e(0)| < k_\theta(0)$. In such a case, it finally follows that

$$|\theta(t)| \leq |\theta_e(t)| + |\theta_c(t)| < k_\theta(t) + |\theta_c(t)| = \frac{\pi}{2} \quad \forall t \geq 0.$$

■

In the second place, Proposition 4 shows that the nominal position error system (19) can be asymptotically stabilized by the proposed force command (23).

PROPOSITION 4 Consider the nominal position error system (19). Suppose that Assumptions 1 and 2 hold. The proposed force command (23) guarantees that $\lim_{t\to\infty} p_e(t) = 0$ and $\lim_{t\to\infty} v_e(t) = 0$.

PROOF Assign a Lyapunov function as follows:

$$L_p = \int_0^{s_p} \mathbf{tanh}^T(\xi)\mathrm{d}\xi + \int_0^{v_e} \mathbf{tanh}^T(\xi)\mathrm{d}\xi + \frac{c_p}{2k_p}\|v_e\|^2. \quad (39)$$

In terms of Lemma 1, it is upper bounded by

$$L_p \leq \chi_1\|\mu_p\|^2 \quad (40)$$

where $\chi_1 = 1/2 + c_p/(2k_p)$ and $\mu_p = [s_p^T, v_e^T]^T$. Differentiating L_p along (19) yields

$$\dot{L}_p = c_p\mathbf{tanh}^T(s_p)v_e + \vartheta_p^T\left(-ge_3 - \ddot{p}_r + u_c + \rho_T + \rho_p\right). \quad (41)$$

Given Assumptions 1 and 2, it follows from Lemma 3 that

$$\vartheta_p^T\rho_T \leq \frac{\bar{\varepsilon}T_n}{m}\sum_{i=x,y,z}|\vartheta_{p,i}| \leq \frac{\bar{\varepsilon}T_n}{m} \times \sum_{i=x,y,z}\left[\vartheta_{p,i}\tanh\left(\frac{\vartheta_{p,i}}{\eta}\right) + k_q\eta\right]$$
$$= \frac{\bar{\varepsilon}T_n}{m}\vartheta_p^T\mathbf{tanh}\left(\frac{\vartheta_p}{\eta}\right) + \frac{3k_q\eta\bar{\varepsilon}T_n}{m}$$
$$\vartheta_p^T\rho_p \leq \vartheta_p^T\mathbf{Tanh}\left(\frac{\vartheta_p}{\eta}\right)\bar{\rho}_p + k_q\eta\|\bar{\rho}_p\|_1.$$

Thus, $\dot{L}_p$ satisfies

$$\dot{L}_p \leq c_p\mathbf{tanh}^T(s_p)v_e + \vartheta_p^T\Bigg(-ge_3 - \ddot{p}_r + u_c + \frac{\bar{\varepsilon}T_n}{m}\mathbf{tanh}\left(\frac{\vartheta_p}{\eta}\right) + \mathbf{Tanh}\left(\frac{\vartheta_p}{\eta}\right)\bar{\rho}_p\Bigg) + \hbar_p\eta \quad (42)$$

where $\hbar_p = 3k_q\bar{\varepsilon}T_n/m + k_q\|\bar{\rho}_p\|_1$. Moreover, by considering (20) and the fact that $\|u_{p,1}\| \leq 3\bar{\varepsilon}\varrho_p/(\sqrt{3}-3\bar{\varepsilon})$, it follows that

$$\vartheta_p^T\left[u_{p,1} + \frac{\bar{\varepsilon}T_n}{m}\mathbf{tanh}\left(\frac{\vartheta_p}{\eta}\right)\right]$$
$$\leq -\frac{\sqrt{3}\bar{\varepsilon}}{\sqrt{3}-3\bar{\varepsilon}}\varrho_p\vartheta_p^T\mathbf{tanh}\left(\frac{\vartheta_p}{\eta}\right) + \bar{\varepsilon}\varrho_p\vartheta_p^T\mathbf{tanh}\left(\frac{\vartheta_p}{\eta}\right) + \|u_{p,1}\|\bar{\varepsilon}\vartheta_p^T\mathbf{tanh}\left(\frac{\vartheta_p}{\eta}\right)$$
$$\leq -\frac{\sqrt{3}\bar{\varepsilon}}{\sqrt{3}-3\bar{\varepsilon}}\varrho_p\vartheta_p^T\mathbf{tanh}\left(\frac{\vartheta_p}{\eta}\right) + \bar{\varepsilon}\varrho_p\vartheta_p^T\mathbf{tanh}\left(\frac{\vartheta_p}{\eta}\right) + \frac{3\bar{\varepsilon}^2}{\sqrt{3}-3\bar{\varepsilon}}\varrho_p\vartheta_p^T\mathbf{tanh}\left(\frac{\vartheta_p}{\eta}\right)$$
$$= 0.$$

Accordingly, substituting the proposed force command (23) into (42) yields

$$\dot{L}_p \leq -k_p\|\mathbf{tanh}(s_p) + \mathbf{tanh}(v_e)\|^2 - c_p v_e^T\mathbf{tanh}(v_e) + \hbar_p\eta$$
$$\leq -\mathbf{tanh}^T(\mu_p)\Lambda\mathbf{tanh}(\mu_p) + \hbar_p\eta \quad (43)$$

where $\Lambda = \begin{bmatrix} k_pI_3 & k_pI_3 \\ k_pI_3 & (k_p+c_p)I_3 \end{bmatrix}$. Since there exists an invertible matrix $M = \begin{bmatrix} I_3 & I_3 \\ 0 & I_3 \end{bmatrix}$ such that $M^{-T}\Lambda M^{-1} = \begin{bmatrix} k_pI_3 & 0 \\ 0 & c_pI_3 \end{bmatrix}$, $\dot{L}_p$ further satisfies

$$\dot{L}_p \leq -\chi_2\|\mathbf{tanh}(\mu_p)\|^2 + \hbar_p\eta$$

where $\chi_2 = \min\{k_p, c_p\}\lambda_{\min}(M^TM)$. On the other hand, in terms of (23a) and (23c), we have that

$$\|\varrho_p\| \leq \|u_{\mathrm{nom}}\| + \|u_{p,2}\| \leq \bar{\varrho}_p$$

where $\bar{\varrho}_p = g + \sup_{t\geq 0}\|\ddot{p}_r(t)\| + 2\sqrt{3}k_p + \|\bar{\rho}_p\|$ is a constant. It then follows from (23b) that $\|u_{p,1}\| \leq 3\bar{\varepsilon}\bar{\varrho}_p/(\sqrt{3}-3\bar{\varepsilon})$. This, from (20), implies that $T_n \leq \sqrt{3}m\bar{\varrho}_p/(\sqrt{3}-3\bar{\varepsilon})$. Motivated by this fact, there is a positive constant $\bar{\hbar}_p$ such that $\hbar_p \leq \bar{\hbar}_p$. It thus follows that

$$\dot{L}_p \leq -\chi_2\|\mathbf{tanh}(\mu_p)\|^2 + \bar{\hbar}_p\eta \leq \bar{\hbar}_p\eta. \quad (44)$$

According to the comparison principle [33], this implies that

$$L_p(t) - L_p(0) \leq \frac{\bar{\hbar}_p}{\alpha}(1 - e^{-\alpha t}) \leq \frac{\bar{\hbar}_p}{\alpha}. \quad (45)$$

This indicates that $L_p \in \mathcal{L}_\infty$ and further that there exists a positive constant $\bar{\mu}_p$ such that $\|\mu_p\| \le \bar{\mu}_p$. In this case, there exists a constant $\chi \in (0, \frac{\tanh(\bar{\mu}_p)}{\bar{\mu}_p})$ such that $\chi\|\mu_p\| \le \|\mathbf{tanh}(\mu_p)\|$ [34]. Next, by considering (40) and the former inequality of (44), it follows that

$$\dot{L}_p \le -\chi_2\chi\|\mu_p\|^2 + \bar{\hbar}_p\eta \le -\bar{\chi}L_p + \bar{\hbar}_p\eta \tag{46}$$

where $\bar{\chi} = \chi_2\chi/\chi_1$. According to the comparison principle [33], this implies that

$$L_p(t) \le \begin{cases} e^{-\bar{\chi}t}L_p(0) + \frac{\bar{\hbar}_p}{\bar{\chi}-\alpha}(e^{-\alpha t} - e^{-\bar{\chi}t}), & \text{if } \alpha \ne \bar{\chi} \\ e^{-\bar{\chi}t}L_p(0) + \frac{\bar{\hbar}_p}{\bar{\chi}}e^{-\bar{\chi}t}t, & \text{if } \alpha = \bar{\chi}. \end{cases}$$

It thus follows that $\lim_{t\to\infty} L_p(t) = 0$ and further that $\lim_{t\to\infty} s_p(t) = 0$ and $\lim_{t\to\infty} v_e(t) = 0$. Finally, due to the definition of s_p, it is trivial to show that $\lim_{t\to\infty} p_e(t) = 0$. ■

In the third place, Proposition 5 shows that the perturbation item $T_n(R - R_c)e_3/m$ in the position error system (18) converges to zero asymptotically.

PROPOSITION 5 Consider the position error system (18). The force command (23) and desired torque (28) guarantee that the perturbation item $T_n(R - R_c)e_3/m$ converges to zero asymptotically.

PROOF It has been shown in the analysis of Proposition 4 that the desired thrust is upper bounded by $T_n \le \bar{T}_n = \sqrt{3}m\bar{\varrho}_p/(\sqrt{3} - 3\bar{\varepsilon})$, which is independent of the system states. Next, define $r_e = (R - R_c)e_3$. Motivated by [9], there exists a positive constant ζ such that $\|r_e\| \le \zeta\|\gamma_e\|$. Since Proposition 3 has shown that $\lim_{t\to\infty} \gamma_e(t) = 0$, we know that $\lim_{t\to\infty} \bar{T}_n r_e(t) = 0$. It therefore follows that $\lim_{t\to\infty} T_n(t)(R(t) - R_c(t))/m = 0$. ■

We next use a theorem to summarize the main results of this article.

THEOREM 1 Consider the VTOL UAV system in (4)–(7) with thrust and torque faults (8) and (9). Suppose that Assumptions 1 and 2 hold. If the initial pitch $\theta(0)$ satisfies (29), the proposed force command (23) and desired torque (28) achieve the trajectory tracking objective in the sense of (15).

PROOF Since Propositions 3–5 have demonstrated conditions Th.i–Th.iii, the asymptotic stability of the error system in (18) and (22) is affirmed. According to Proposition 1, this guarantees that the trajectory tracking of the VTOL UAV system in (4)–(7) with thrust and torque faults in (8) and (9) is achieved in the sense of (15). ■

V. SIMULATIONS

Consider a VTOL UAV with the inertia parameters $m = 0.85\,\text{kg}$ and $J = \text{diag}\{4.856, 4.856, 8.801\} \times 10^{-3}\text{kg}\cdot\text{m}^2$. Suppose that the VTOL UAV is equipped with global positioning system and inertial measurement unit sensors such that its position, velocity, attitude, and angular velocity can be measured without noise. Some simulations are carried out in the following to validate and highlight the developed control algorithm.

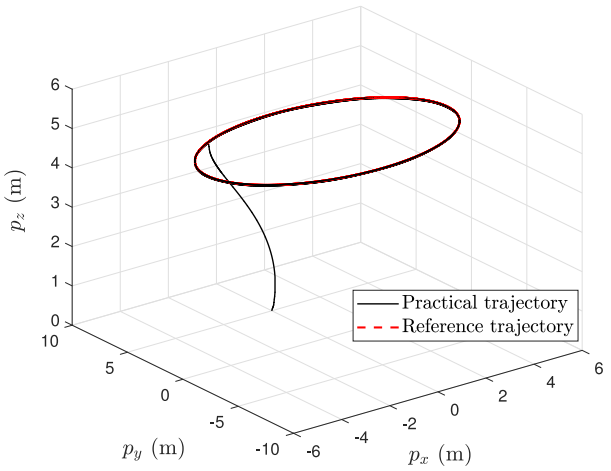

Fig. 1. Three-dimensional trajectory tracking snapshot.

A. Performance Verification

In this scenario, the VTOL UAV is commanded to track reference trajectory and yaw specified as $p_r = [5\cos(0.2t), 5\sin(0.2t), 5]^T\,\text{m}$ and $\psi_r = \pi/3\text{rad}$. Affected by gust wind, the VTOL UAV system is assumed to suffer from disturbance thrust and torque in the form of

$$\begin{aligned} d_f &= [0.5\cos(0.2t), 0.4\exp(-0.2t), 0.2\sin(0.1t)] \\ d_\tau &= [0.3\sin(0.4t), 0.2\cos(0.2t), 0.1\exp(-0.1t)]. \end{aligned} \tag{47}$$

Since the overall closed-loop VTOL UAV error system is in terms of a hierarchical framework composed of an inner attitude loop and an outer position loop, it had better make the prior stability of the inner attitude loop in order for the stability of the outer position loop. Motivated by this fact, we choose the attitude control parameters $c_a = 12$ and $k_a = 12$ larger than the position control parameters $c_p = 8$ and $k_p = 4$. In addition, we choose the upper bound constants $\bar{\varepsilon} = 0.5$, $\bar{\epsilon} = 0.8$ (based on Assumption 1), $\bar{\rho}_p = [5, 5, 5]^T$ and $\bar{\rho}_a = [5, 5, 5]^T$ in terms of a tradeoff between the desirable robustness against disturbances and actuator faults and the adverse chattering. The VTOL UAV is initialized as $p(0) = [0, 5, 0]^T\,\text{m}$ and $\gamma(0) = [0, 0, 0]^T\,\text{rad}$ without motion. In addition, to verify the robustness of the proposed control algorithm against the actuator faults, suppose that there is a sudden loose in the component of some rotor of the studied VTOL UAV at 30 s such that the rotor begins to wobble. This sudden event is assumed to bring 30% reduction in the applied force, 40% reduction in the applied torque, as well as force and torque biases formulated by

$$\begin{aligned} T_d &= 0.4\sin(2t + 0.2) - 0.4\exp(-0.3t) \\ \tau_d &= \begin{bmatrix} 0.4\cos(0.5t - 0.5) - 0.4\exp(-0.03t) \\ \exp(-0.08t) - \sin(t + 0.2) \\ \cos(-0.01t) - \sin(-0.1t) \end{bmatrix}. \end{aligned} \tag{48}$$

The simulation results are illustrated in Figs. 1–3.

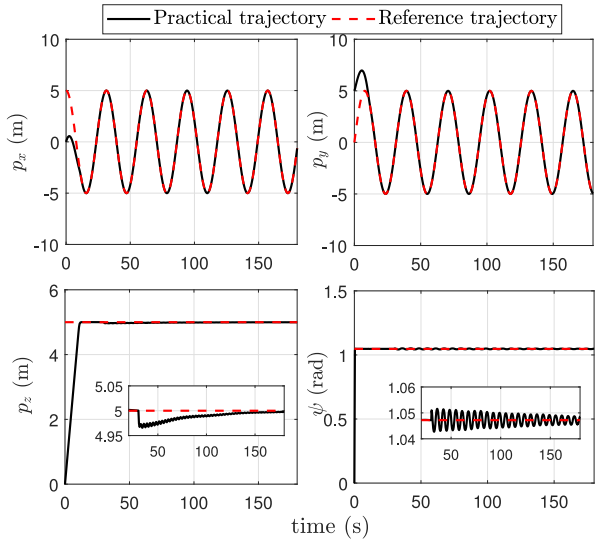

Fig. 2. Position and yaw trajectories with respect to reference ones.

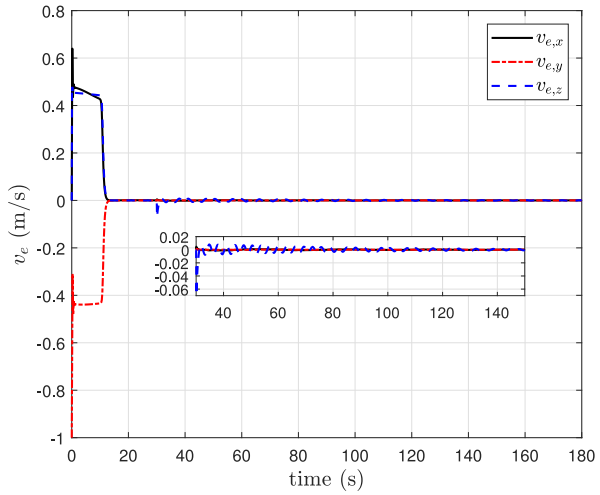

Fig. 3. Velocity tracking errors.

Fig. 1 displays the practical trajectory of the VTOL UAV with respect to the reference one. It can be seen that the trajectory tracking objective is achieved by the developed control algorithm in spite of the actuator faults and disturbances. Specifically, it can be seen from Fig. 2 that the position and yaw asymptotically converge to their reference ones before 30 s when the sudden fault leads to the recurrence of the tracking errors. Still, the proposed control algorithm guarantees the asymptotic convergence of the position and yaw to their reference ones after 30 s. Moreover, Fig. 3 exhibits that the velocity error asymptotically converges to zero in spite of the sudden fault. In addition, Fig. 4 depicts the bounded applied force and torque. However, it can be observed that, to counteract the fault effect, some oscillation is introduced. Note that such oscillation is of small amplitude, which is tolerable in real maneuvers.

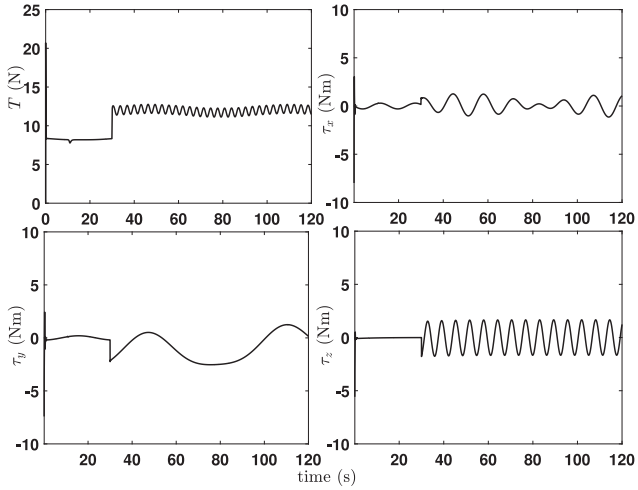

Fig. 4. Applied force and torque.

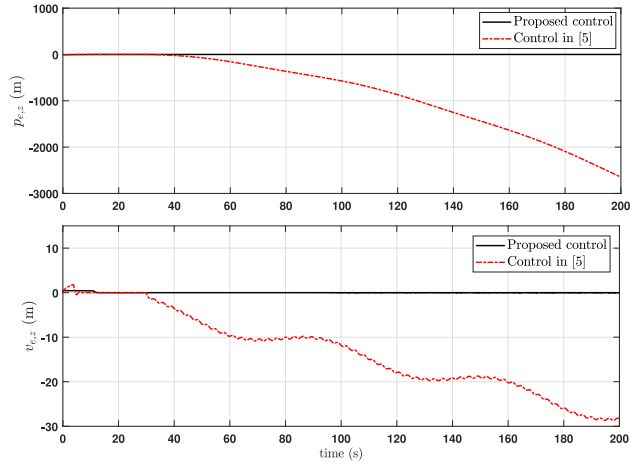

Fig. 5. Position error comparison.

B. Robustness Comparison

To highlight the robust performance of the proposed control algorithm, we compare it with the one in [7] without the fault-tolerant mechanism. In this scenario, the VTOL UAV is commanded to hover at $p_r = [0, 0, 5]^T$ m with $\psi_r = 0$ rad. Suppose that it is subject to the same fault event, as described in the previous scenario. Also, the parameters we need are identical with those in the previous scenario. The VTOL UAV initially rests at $p(0) = [-5, 5, 0]^T$ m with $\gamma(0) = [0, 0, 0]^T$ rad. For clarity, we take the position and velocity errors on axis z_I resulting from two control algorithms for a comparison. In particular, Fig. 5 shows the comparison result. It can be observed that the position and velocity errors driven by the robust control algorithm asymptotically converge to zero in spite of a sudden fault. However, the position and velocity errors driven by the control algorithm in [7] without robustness diverge to negative infinity arising from the actuator fault. By comparison, we know that the proposed control algorithm is of great robustness against actuator faults.

VI. CONCLUSION

A robust fault-tolerant control algorithm is proposed for VTOL UAVs subject to thrust and torque faults as well as disturbances such that it is able to track reference trajectory and yaw. In terms of the hierarchical framework, we survey the position and attitude loops separately. By combining a saturation control technique with a robust fault-tolerant strategy, a force command is first developed for the position tracking. Subsequently, by implementing the similar robust fault-tolerant strategy, a desired torque with a proper initial condition is synthesized for the nonsingular attitude tracking. It has been shown with hierarchical system stability theory that the asymptotically stable trajectory tracking of the VTOL UAV is fulfilled by using the developed control algorithm. In the future, we will verify the effectiveness of the proposed control algorithm on a real experiment platform.

APPENDIX A
PROOF OF PROPOSITION 2

It is trivial that the inequalities in (24) are sufficient for the validity of (25). Define $\bar{u}_c = [\bar{u}_{c,x}, \bar{u}_{c,y}, \bar{u}_{c,z}]^T = u_{\text{nom}} + u_{p,2}$. If k_p satisfies (25), it follows from (23) that

$$\begin{aligned}\bar{u}_{c,z} &> g - \sup_{t\geq 0}|\ddot{p}_{r,z}(t)| - 2k_p - \|\bar{\rho}_p\| \\ &> \varsigma\left(\sup_{t\geq 0}\|\ddot{\bar{p}}_r(t)\| + 2\sqrt{2}k_p + \|\bar{\rho}_p\|\right). \end{aligned} \tag{49}$$

By virtue of the definition of ς, this further guarantees that

$$\bar{u}_{c,z} > \frac{\sqrt{3}\bar{\varepsilon}}{\sqrt{3}-3\bar{\varepsilon}}\sqrt{\bar{u}_{c,z}^2 + \left(\sup_{t\geq 0}\|\ddot{\bar{p}}_r(t)\| + 2\sqrt{2}k_p + \|\bar{\rho}_p\|\right)^2}. \tag{50}$$

By using this fact, it finally follows from (23) that

$$\begin{aligned} u_{c,z} &> \bar{u}_{c,z} - \frac{\sqrt{3}\bar{\varepsilon}}{\sqrt{3}-3\bar{\varepsilon}}\varrho_p \\ &> \bar{u}_{c,z} - \frac{\sqrt{3}\bar{\varepsilon}}{\sqrt{3}-3\bar{\varepsilon}} \\ &\quad\times\sqrt{\bar{u}_{c,z}^2 + \left(\sup_{t\geq 0}\|\ddot{\bar{p}}_r(t)\| + 2\sqrt{2}k_p + \|\bar{\rho}_p\|\right)^2} \\ &> 0. \end{aligned} \tag{51}$$

REFERENCES

[1] A. Abdessameud and A. Tayebi
Global trajectory tracking control of VTOL-UAVs without linear velocity measurements
Automatica, vol. 46, no. 6, pp. 1053–1059, 2010.

[2] L. R. G. Carrillo, G. R. F. Colunga, G. Sanahuja, and R. Lozano
Quad rotorcraft switching control: An application for the task of path following
IEEE Trans. Control Syst. Technol., vol. 23, no. 4, pp. 1255–1267, Jul. 2014.

[3] W. He, T. Meng, X. He, and C. Sun
Iterative learning control for a flapping wing micro aerial vehicle under distributed disturbances
IEEE Trans. Cybern., vol. 49, no. 4, pp. 1524–1535, Apr. 2019.

[4] W. He, Z. Yan, C. Sun, and Y. Chen
Adaptive neural network control of a flapping wing micro aerial vehicle with disturbance observer
IEEE Trans. Cybern., vol. 47, no. 10, pp. 3452–3465, Oct. 2017.

[5] M. Hua, T. Hamel, P. Morin, and C. Samson
Introduction to feedback control of underactuated VTOL vehicles: A review of basic control design ideas and principles
IEEE Control Syst. Mag., vol. 33, no. 1, pp. 61–75, Feb. 2013.

[6] L. Wang and H. Jia
The trajectory tracking problem of quadrotor UAV: Global stability analysis and control design based on the cascade theory
Asian J. Control, vol. 16, no. 2, pp. 574–588, 2014.

[7] Z. Zuo and C. Wang
Adaptive trajectory tracking control of output constrained multi-rotors systems
IET Control Theory Appl., vol. 8, no. 13, pp. 1163–1174, 2014.

[8] P. Simplicio, M. D. Pavel, E. V. Kampen, and Q. P. Chu
An acceleration measurements-based approach for helicopter nonlinear flight control using incremental nonlinear dynamic inversion
Control Eng. Pract., vol. 21, no. 8, pp. 1065–1077, 2013.

[9] B. Zhao, B. Xian, Y. Zhang, and X. Zhang
Nonlinear robust sliding mode control of a quadrotor unmanned aerial vehicle based on immersion and invariance method
Int. J. Robust Nonlinear Control, vol. 25, no. 18, pp. 3714–3731, 2014.

[10] B. Zhao, B. Xian, Y. Zhang, and X. Zhang
Nonlinear robust adaptive tracking control of a quadrotor UAV via immersion and invariance methodology
IEEE Trans. Ind. Electron., vol. 62, no. 5, pp. 2891–2902, May 2015.

[11] Y. Zou and Z. Meng
Immersion and invariance-based adaptive controller for quadrotor systems
IEEE Trans. Syst., Man, Cybern.: Syst., vol. 49, no. 11, pp. 2288–2297, Nov. 2019.

[12] G. Raffo, M. Ortega, and F. Rubio
An integral predictive/nonlinear H_∞ control structure for a quadrotor helicopter
Automatica, vol. 46, no. 1, pp. 29–39, 2010.

[13] Y. Zou, Z. Zhou, X. Dong, and Z. Meng
Distributed formation control for multiple vertical takeoff and landing UAVs with switching topologies
IEEE/ASME Trans. Mechatronics, vol. 23, no. 4, pp. 1750–1761, Aug. 2018.

[14] Y. Zou and Z. Meng
Coordinated trajectory tracking of multiple vertical take-off and landing UAVs
Automatica, vol. 99, pp. 33–40, 2019.

[15] X. Dong, Y. Zhou, Z. Ren, and Y. Zhong
Time-varying formation tracking for second-order multi-agent systems subjected to switching topologies with application to quadrotor formation flying
IEEE Trans. Ind. Electron., vol. 64, no. 6, pp. 5014–5024, Jun. 2017.

[16] M. Okasha and B. Newman
Switching algorithm to avoid attitude representation singularity
In *Proc. AIAA Atmos. Flight Mech. Conf.*, Chicago, IL, USA, 2009, pp. 10–17.

[17] S. Taki and D. Nenchevh
Euler angle based feedback control of large eigenaxis rotations in the presence of singularities and model uncertainty
In *Proc. 13th Int. Conf. Control, Autom., Syst*, Gwangju, South Korea, 2013, pp. 34–39.

[18] H. Noura, D. Theilliol, J. C. Ponsart, and A. Chamseddine
Fault-Tolerant Control Systems. London, U.K.: Springer-Verlag, 2009.

[19] M. Staroswiecki, D. Berdjag, B. Jiang, and K. Zhang
PACT: A PAssive/ACTive approach to fault tolerant stability under actuator outages
In *Proc. 48h IEEE Conf. Decis. Control/28th Chin. Control Conf.*, Shanghai, China, 2009, pp. 7819–7824.

[20] J. Cieslak, D. Zolghadri, A. Goupil, and D. Henry
Development of an active fault-tolerant flight control strategy
J. Guid. Control Dyn., vol. 31, no. 1, pp. 135–147, 2008.

[21] Q. Hu, B. Xiao, and M. I. Friswell
Robust fault-tolerant control for spacecraft attitude stabilization subject to input saturation
IET Control Theory Appl., vol. 5, no. 2, pp. 271–282, Jan. 2011.

[22] Y. Wang, B. Jiang, N. Lu, and J. Pan
Hybrid modeling based double-granularity fault detection and diagnosis for quadrotor helicopter
Nonlinear Anal. Hybrid Syst., vol. 21, pp. 22–36, 2016.

[23] H. Yang, B. Jiang, Y. Yang, and K. Zhang
Cooperative control reconfiguration in multiple quadrotor systems with actuator faults
IFAC-PapersOnLine, vol. 48, no. 21, pp. 386–391, 2015.

[24] K. P. B. Chandra, H. Alwi, and C. Edwards
Fault Reconstruction for a quadrotor using an LPV sliding mode observer
IFAC-PaperOnLine, vol. 48, no. 21, pp. 374–379, 2015.

[25] A. Chamseddine, D. Theilloil, Y. Zhang, and C. Join
Active fault-tolerant control system design with trajectory replanning against actuator faults and saturation: Application to a quadrotor unmanned aerial vehicle
Int. J. Adapt. Control Signal Process., vol. 29, pp. 1–23, 2015.

[26] X. Zhang, T. Parisini, and M. M. Polycarpou
Adaptive fault-tolerant control of nonlinear uncertain systems: An information-based diagnostic approach
IEEE Trans. Autom. Control, vol. 49, no. 8, pp. 1259–1274, Aug. 2004.

[27] Y. Zou
Singularity-free adaptive fault-tolerant trajectory tracking controller for VTOL UAVs
Int. J. Syst. Sci., vol. 48, no. 10, pp. 2223–2234, 2017.

[28] R. Ortega, P. J. Nicklasson and H. Sira-Ramirez
Passivity-Based Control of Euler-Lagrange Systems: Mechanical, Electrical, and Electromechanical Applications. New York, NY, USA: Springer-Verlag, 1998.

[29] M. Chen, S. Ge, and B. Ren
Adaptive tracking control of uncertain MIMO systems with input constraints
Automatica, vol. 47, no. 3, pp. 452–465, 2011.

[30] M. Shuster
A survey of attitude representations
J. Astronaut. Sci., vol. 41, no. 4, pp. 439–517, 1993.

[31] A. Abdessameud and A. Tayebi
Motion Coordination for VTOL Unmanned Aerial Vehicles. London, U.K.: Springer, 2013.

[32] H. Yang, B. Jiang, M. Staroswiecki, and Y. Zhang
Fault recoverability and fault tolerant control for a class of interconnected nonlinear systems
Automatica, vol. 54, pp. 49–55, 2015.

[33] H. K. Khalil
Nonlinear Systems, 3rd ed. Englewood Cliffs, NJ, USA: Prentice-Hall, 2002.

[34] B. Zhu and W. Huo
Nonlinear control for a model-scaled helicopter with constraints on rotor thrust and fuselage attitude
Acta Automatica Sinica, vol. 40, no. 11, pp. 2654–2664, 2014.

Yao Zou received the B.S. degree in automation from the Dalian University of Technology, Dalian, China, in 2010, and the Ph.D. degree in control science and engineering from Beihang University (BUAA), formerly named Beijing University of Aeronautics and Astronautics, Beijing, China, in 2016.

He was a Postdoctoral Research Fellow with the Department of Precision Instrument, Tsinghua University, Beijing, from 2017 to 2018. He is currently an Associate Professor with the School of Automation and Electrical Engineering, University of Science and Technology Beijing, Beijing. His current research interests include nonlinear control, unmanned aerial vehicle control, and multiagent control.

Kewei Xia received the Ph.D. degree in control theory and applications from Beihang University, Beijing, China, in 2017.

He was a Postdoctoral Fellow with the Yonsei University Observatory, Yonsei University, Seoul, South Korea, from 2017 to 2018. He is currently a Postdoctoral Researcher with the School of Mechanical, Aerospace and Nuclear Engineering, Ulsan National Institute of Science and Technology, Ulsan, South Korea. His current research interests include nonlinear control, spacecraft control, and unmanned aerial vehicle control.